Paper 27

12th Symposium on Measuring Techniques
for Transonic and Supersonic Flow in Cascades and Turbomachines

Prague, Czech Republic, September 12-13,1994

NON INTRUSIVE MEASUREMENTS OF THE UNSTEADY FLOW IN THE RADIAL GAP BETWEEN CENTRIFUGAL IMPELLER AND VANED DIFFUSER

M. Ubaldi, P. Zunino, G. Barigozzi, A. Ghiglione
Universita di Genova
Italy

NON-INTRUSIVE MEASUREMENTS OF THE UNSTEADY FLOW IN THE RADIAL GAP BETWEEN CENTRIFUGAL IMPELLER AND VANED DIFFUSER

Marina Ubaldi, Pietro Zunino, Giovanna Barigozzi, Andrea Ghiglione

Istituto di Macchine e Sistemi Energetici
Università di Genova (Italy)

ABSTRACT

The paper describes the model, the instrumentation and the experimental procedure developed to study the upstream effect of the vaned diffuser on the centrifugal impeller outflow.

A detailed investigation of the unsteady kinematic characteristics of the flow in the narrow radial gap between impeller and diffuser and in the rear part of the impeller rotating passages has required the use of a non intrusive laser Doppler technique.

The data reduction technique developed to reconstruct sequences of images of the flow perturbed by the diffuser from measurements taken in the absolute frame of reference is discussed. Examples of the obtained results, which show the main features of the phenomenon investigated, are given.

NOMENCLATURE

c	absolute velocity
D_2	impeller outlet diameter
l	chord length
p_t	total pressure
Q	flow rate
r	radial coordinate
t	time
Tu	random unsteadiness
T_i	impeller blade passing period
U_2	peripheral velocity at the impeller outlet
w	relative velocity
y	circumferential coordinate in the relative frame
z	axial coordinate
z_d	number of diffuser vanes
z_i	number of impeller blades
ν	kinematic viscosity
ρ	fluid density
ϑ	angular coordinate
φ	flow rate coefficient $\varphi = 4Q/(U_2 \pi D_2^2)$
ψ	total pressure rise coefficient $\psi = 2(p_{t4} - p_{t0})/(\rho U_2^2)$
ω	angular velocity

Subscripts

r	in the radial direction
u	in the tangential direction
0	in the suction pipe
1	at the impeller leading edge
2	at the impeller outlet
3	at the diffuser inlet
4	at the diffuser outlet

Superscripts

'	unsteady quantity
~	ensemble average
—	circumferential average

1. INTRODUCTION

Rotor-stator aerodynamic interaction is a major cause of flow unsteadiness in turbomachinery. The phenomenon takes place through two distinct mechanisms:

- the effect of the impact, transport and mixing of the wakes of the preceding blade row on the downstream row in relative motion;
- the potential flow effect due to the interaction of the inviscid flow field created by the blade rows in relative motion, which influences the flow both in downstream and upstream directions.

The first effect, being proved to be the most important one, has been extensively investigated (e. g. [1-6]). The second mechanism becomes important when the distance between the blade rows is reduced, as in modern centrifugal pumps and compressors with vaned diffusers.

Recently the authors have investigated the upstream effect of the vaned diffuser on the impeller outflow in a centrifugal turbomachine [7]. Velocity measurements have been taken by means of a hot wire probe placed in the radial gap between the impeller and the vaned diffuser. Furthermore the unsteady pressure field in the gap and in the impeller has been surveyed by means of miniature fast response pressure transducers flush mounted on the fixed endwall faced to the unshrouded impeller. A more detailed study of the flow in the radial gap, in proximity of the impeller blades and in the rear part of the impeller passages, requires the use of non intrusive

Table 1 Geometric data and operating conditions

Impeller			
inlet blade diameter	D_1 =	240	mm
outlet diameter	D_2 =	420	mm
blade span	b =	40	mm
number of blades	z_i =	7	
Diffuser			
inlet vane diameter	D_3 =	444	mm
outlet vane diameter	D_4 =	664	mm
vane span	b =	40	mm
number of vanes	z_d =	12	
Operating conditions			
rotational speed	n =	2000	rpm
flow rate coefficient	φ =	0.048	
total pressure coefficient	ψ =	0.65	
Reynolds number	Re =	$U_2 l/\nu$	$= 6.5\ 10^5$
Inlet air reference conditions			
temperature	T =	298	K
air density	ρ =	1.2	Kg/m^3

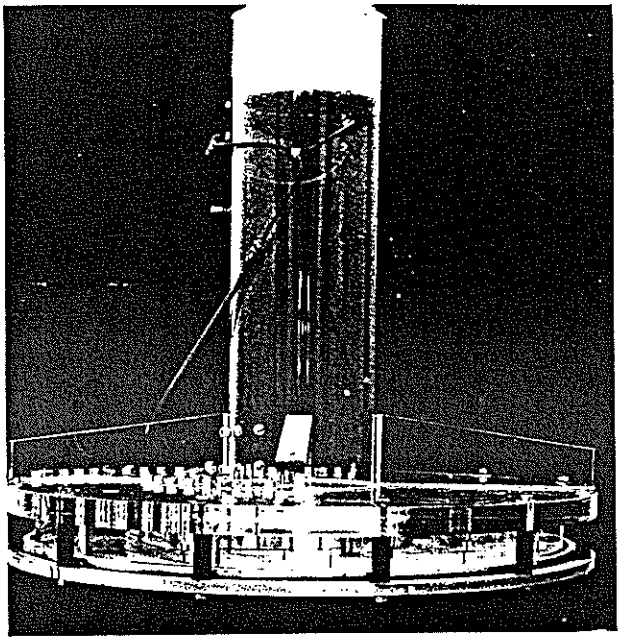

Fig. 1 Centrifugal turbomachine model

techniques. The present paper describes an application of the laser Doppler velocimetry to the experimental study of this unsteady flow.

2. EXPERIMENTAL APPARATUS

A centrifugal turbomachine model suitable for detailed flow investigations has been used during the present study. The model, shown in fig. 1, is described in details in [7].

The model operates in an open circuit. The flow enters the model at the atmospheric conditions through a long vertical straight pipe equipped with a honeycomb, a filtering section, and a throttle valve to control the operating point and it is discharged from the vaned diffuser directly into the atmosphere. The suction pipe is connected to a thick plexiglas disk, which constitutes the upper endwall of the casing for the impeller and diffuser passages, which have a constant axial width of 40 mm. The tip clearance between blades and casing, which can be varied, is set in the present experiment at its minimum value of 0.4 mm.

The impeller is directly driven by a vertical axis electric d. c. motor which allows a continuous variation of the rotational speed.

The casing is instrumented with flush mounted pressure transducers, probe holders and a rectangular glass window (300 x 100 x 3 mm) which provides the optical access of the laser beams to large part of the internal impeller passages and to the radial gap between rotor and stator.

The centrifugal stage consists of the unshrouded impeller 420 mm diameter equipped with seven simple curvature backward blades followed by twelve diffuser vanes (fig. 2). The radial gap between rotor and stator of 6 per cent of the impeller outlet radius is typical of modern centrifugal turbomachines.

The roots of the diffuser vanes are fixed on a ring which is allowed to rotate for modifying the relative position of the probe volume, respect to the diffuser vanes. That makes possible a detailed circumferential investigation of the absolute unsteady flow in the radial gap.

The experiment was conducted at a constant rotational speed of 2000 rpm, at the nominal operating point: flow coefficient $\varphi = 0.048$, total pressure rise coefficient $\psi = 0.65$.

The main geometrical data of the model and the operating conditions are summarised in tab. 1. The coordinates of the impeller blade and diffuser vane profiles are given in ref. [7].

3. INSTRUMENTATION AND MEASURING PROCEDURE

A dual beam laser fringe velocimeter with on-axis back scatter collection optics was used for the present investigation. The light was supplied by a 35 mW Helium - Neon laser operating at 632.8 nm. A focusing lens with 310 mm focal length and a beam expander with 1.94 expansion ratio provide a beam intersection half

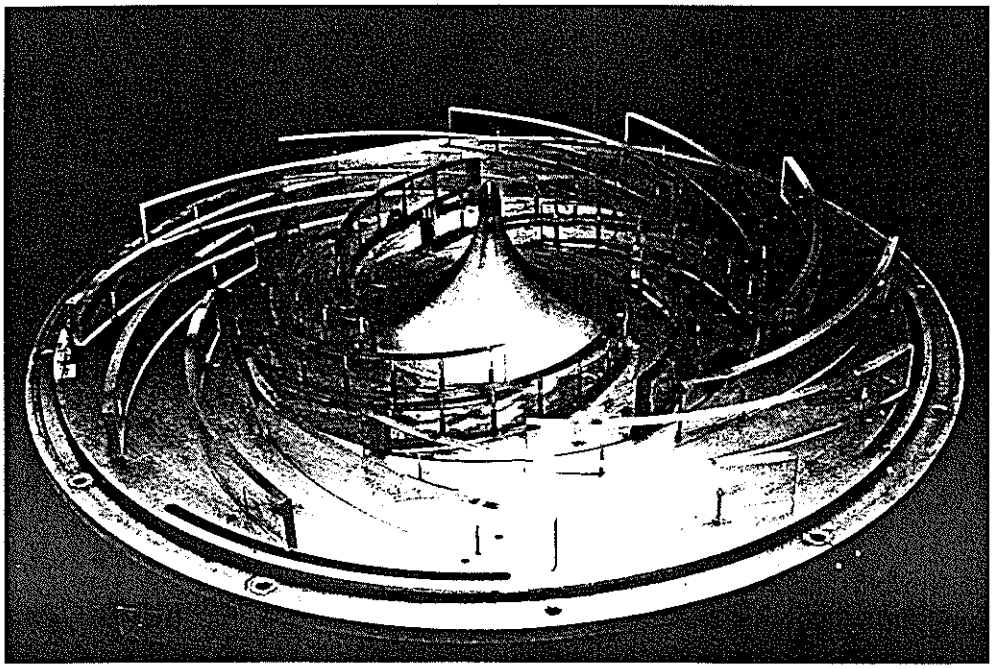

Fig. 2 Unshrouded radial impeller and vaned diffuser

angle of 6.7 deg and a probe volume of 0.1 x 0.1 x 1 mm, based on the $1/e^2$ intensity boundary. A Bragg cell with a frequency shift of 40 MHz was used to solve the directional ambiguity and to reduce the measuring error due to the angular bias. The optical system is mounted on a manual three axis traversing table with a resolution of 0.1 mm.

In the present investigation the optical axis, which is horizontal, was aligned in the radial direction and a plane mirror mounted on a two axis precision translation stage fixed on the model casing was used to steer the beams 90 deg to enter the impeller passage parallel to the axial direction. Therefore, by rotation of the optics, the components of the absolute velocity in the blade-to-blade plane can be measured. Combined translations of the main optics along the optical axis and the steering mirror in radial direction determine a radial movement of the probe volume at constant axial position. The circumferential traversing is obtained by rotation of the diffuser ring.

The flow was seeded with an atomised spray of mineral oil generated by a home made air atomiser. The mean diameter of the particles was less than 2 μm and therefore, according to the analyses of Adrian [8] and Dring [9], it can be considered adequate to follow flow fluctuations due to the blade passing frequencies, the rotor-stator interaction and the vortices containing large turbulence energy (maximum absolute velocity 40 m/s, blade passing frequency 233 Hz).

The seeding was injected into the flow upstream of the inlet pipe in order to minimise flow disturbances. The signal frequencies from the photo multiplier were measured by means of a Dantec 55L90a counter processor used in 5/8 fringe count mode.

4. DATA PROCESSING AND RESULTS

Data sampling

As the arrival time of the particles was not available at the digital output of the counter processor, information on both fringe crossing frequency and corresponding arrival time was obtained by fast sampling the analog output signal of the counter. An one per revolution signal obtained from the rotor disk was used to trigger the A/D converter that sampled the input signal at a frequency of 14 kHz until 180 data, corresponding to 180 circumferential positions across three consecutive blade passages, were collected.

This procedure is efficient, as it allows free running of the laser velocimeter and contemporaneous acquisition of a position information used to assign each instantaneous velocity measurement to the proper circumferential location relative to the impeller blades.

The counter processor output signal is stepwise. During the time interval between two successive passages of particles in the probe volume, the signal is constant and proportional to the fringe crossing frequency of the first particle; only when a new seeding particle crosses the probe volume the signal level is updated.

As the typical counter validated data rate is 200 Hz and the sampling rate is 14 kHz, a mean of 70 samples is taken in the interval between two successive particle passages in the probe volume. A subroutine of the data acquisition program has been developed which checks the data: a sampled datum is considered valid only if the counter has processed a new measurement during the sampling interval and the validated datum is assigned to the position corresponding to the center of the sampling interval.

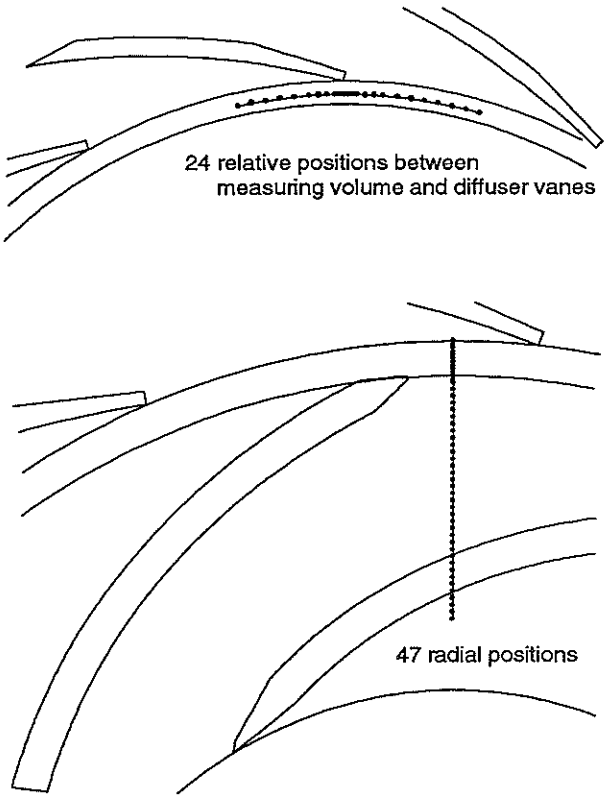

Fig. 3 Measuring points

Ensemble averaging

Ensemble averaging procedure was applied to the phase locked instantaneous valid data collected, in order to separate the periodic component of the signal at the blade passing frequency from the random component due to turbulence, vortex shedding and all other fluctuations not correlated with the rotor speed. The ensemble average was performed over 30000 impeller revolutions which, with a typical counter data rate of 200 Hz, yield an average of 428 data for each circumferential position, according to the following relationship:

$$\tilde{S} = (D \cdot R \cdot 60) / (n \cdot z_i \cdot p)$$

where $\tilde{S}$ mean validated samples, D data rate, R number of impeller revolutions, n revolutions per minute, z_i number of impeller blades, p number of points per impeller blade passage.

At a fixed axial (z) and radial (r) position in the absolute frame of reference, the instantaneous velocity c is a function of time (t_j) or order of the sampled signal in the record, of the record n to be ensemble averaged and of the circumferential position of the probe volume with respect to the diffuser vane (ϑ_k):

$$c(t_j, \vartheta_k, n) = \tilde{c}(t_j, \vartheta_k) + c'(t_j, \vartheta_k, n)$$

The ensemble averaged velocity is:

$$\tilde{c}(t_j, \vartheta_k) = \frac{1}{N} \sum_{n=1}^{N} c(t_j, \vartheta_k, n)$$

and the ensemble averaged random unsteadiness:

$$\sqrt{\tilde{c'^2}(t_j, \vartheta_k)} = \sqrt{\frac{1}{N} \sum_{n=1}^{N} \left[c(t_j, \vartheta_k, n) - \tilde{c}(t_j, \vartheta_k) \right]^2}$$

In the relative frame of reference the upstream stator effect is seen as a periodic disturbance at the stator vane passing relative frequency, perturbing the non uniform quasi steady flow. In the absolute frame of reference the stator effect results in a different distribution of the periodic impeller outflow seen by the observer when he changes its circumferential position with respect to the diffuser.

The flow has been surveyed at 47 radial positions in a blade-to-blade plane located at the blade mid-span. To study the diffuser effect on the impeller flow, for each radial position, ensemble averaged distributions of 180 data at 24 different circumferential positions of the measuring volume have been produced. Measuring locations are shown in fig. 3

Ensemble averaged mean and rms velocity components taken at R = 214 mm (in the radial gap 4 mm downstream of the blade trailing edge, 8 mm upstream of the vane leading edge) and ϑ/ϑ_d = 0.065 (position nearly circumferentially centered in the diffuser passage) are shown in fig. 4. From left to right the instrument in sequence senses the impeller pressure side, the wake, the suction side, the mid-passage and then the pressure side again.

The diagrams display good periodicity and continuous and smooth distributions.

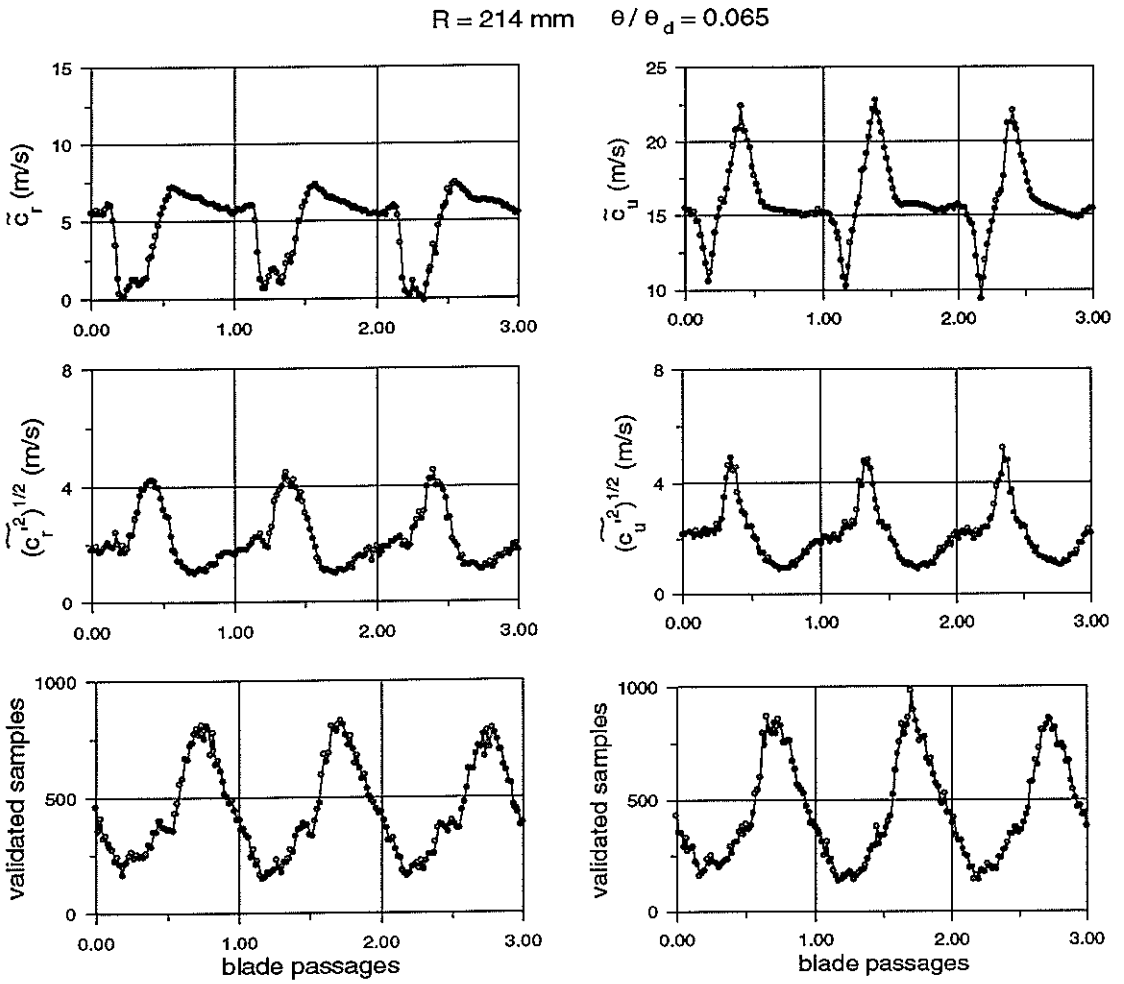

Fig. 4 Ensemble averaged mean and rms velocity components

The radial velocity shows a large defect in the wake, while the tangential velocity experiences an abrupt variation through the wake. Both radial and tangential rms velocities present important peaks on the suction side of the wakes. On the bottom of fig. 4, the distributions of the validated samples along the blade passages show that, against an expected mean value of about 400 data, peaks of 800 data are present in the mid-passages, while only 200 data are collected in the blade wakes. The collected validated samples are strongly correlated with the velocity distributions and therefore very large statistical bias affects the unweighted time average of the velocity. On the contrary, ensemble averaged velocities are free from this statistical bias associated with the rotor induced periodic unsteadiness, but should suffer only the statistical error induced by the random unsteadiness.

Error estimate

Sources of errors associated with LDV velocity measurements have been widely discussed in literature. Comprehensive reviews for turbomachinery applications with guide lines for error evaluation are given by Strazisar and Powell [10] and Strazisar [11].

The error on the ensemble averaged velocity depends on the ratio of the standard deviation $\tilde{\sigma}$ with the mean velocity $\tilde{c}$ and on the number of samples $\tilde{S}$ used for averaging, according to the following formula for a 95 per cent confidence level: $\varepsilon = \pm 2\tilde{\sigma} / (\tilde{c}\sqrt{\tilde{S}})$.

Counter processor errors due to random optical and electronic noise, quantization and synchronisation errors and flow velocity fluctuations contribute to increase the standard deviation.

Optical and electronic noise are minimised by the use of high quality components, accurate alignment of the optics, optical glass window and non reflecting painting of background surfaces. Furthermore the present measurements were performed at mid-span, 20 mm from the two endwall, where effects of light reflected by solid surfaces are negligible and the photo multiplier signal to noise ratio is high (typically larger than 10:1).

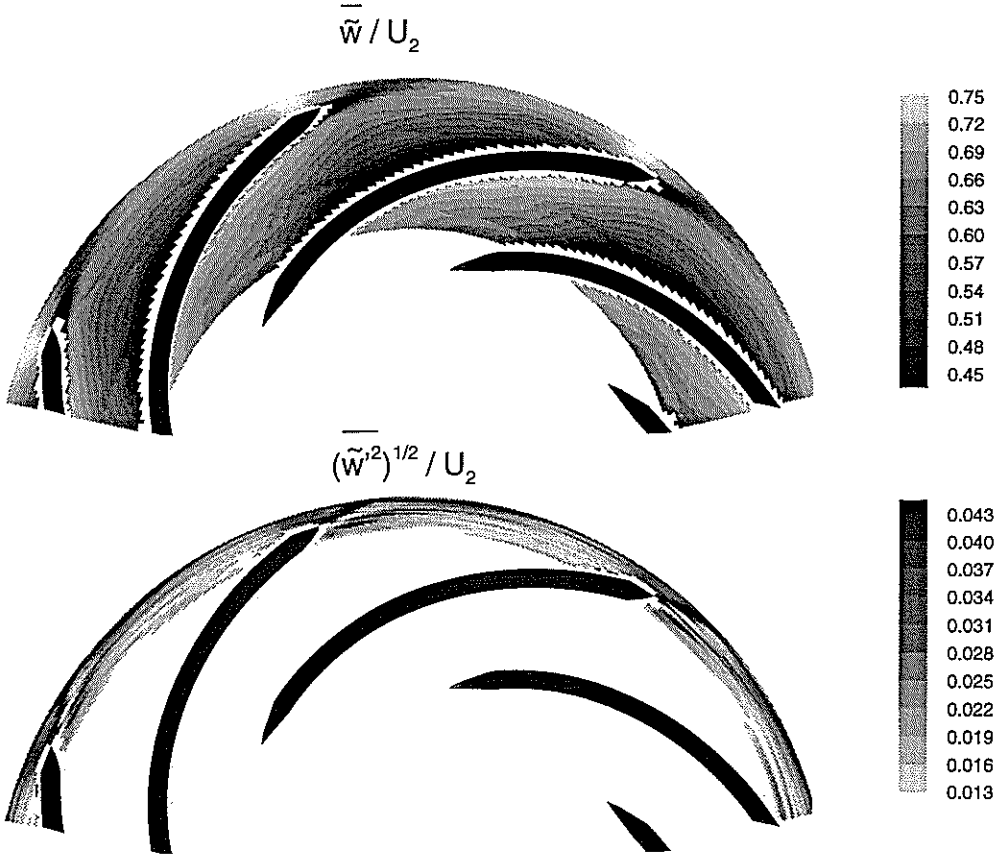

Fig. 5 Circumferentially averaged relative velocity and relative velocity stator generated unsteadiness

With a signal to noise ratio larger than 5:1 and signal frequencies lower than 40 MHz, the counter processor error is lower than 1 per cent of the velocity. Quantization error due to the 8 bit counter processor D/A converter is less than 0.4 per cent of the span. The errors due to the 12 bit A/D converter of the data acquisition system, the flow fluctuations caused by drift in rotor speed, the velocity variations due to velocity gradients in the probe volume and in the sampling interval are considered to be negligible.

The largest contribution to the standard deviation is the unresolved flow unsteadiness, in large part associated with turbulence. An estimate of the overall error due to finite sampling indicates values lower than 2 per cent for both radial and circumferential velocity in most of the flow field. However, for few points in the wake, where contemporaneously the radial velocity decreases and the number of validated samples is reduced, the error becomes larger than 10 per cent.

As previously observed, the ensemble averaging technique avoids the statistical bias caused by the strong correlation between periodic velocity variations associated with the impeller rotation and the data sampling distribution. A statistical error can only be introduced by velocity fluctuations due to random unsteadiness. In this case the correlation with the number of samples per unit time is less clear and no attempt of correction has been tried. According to Strazisar [11], the error depends on the ratio between the kinetic energy of the fluctuations and kinetic energy of mean flow. This effect has been estimated to be lower than 1 per cent in most of the flow field, but for the radial component it becomes larger than 10 per cent in part of the wake region.

Angular bias occurs when the velocity direction fluctuates in time. More measurements per unit time are taken when the velocity direction is normal to the fringe pattern, less when the velocity deviates from this direction. The use of the Bragg cell to shift of 40 MHz one of the two beams makes the fringe pattern to move in the measuring volume with a velocity of about 110 m/s. In this way the angular variation of the velocity relatively to the fringe pattern is reduced to less than 15 deg, even in the wake region where the angle of the absolute velocity can deviate locally of 90 deg. According to Strazisar and Powell [10] the error due to angular bias is less than 1 per cent for angular variations lower than 20 deg.

Stator generated unsteadiness

Following the procedure proposed in [7] the ensemble averaged distributions obtained for the different circumferential locations are circumferentially averaged in phase to obtain a velocity distribution, independent on the circumferential location of the probe volume, which is representative of the impeller mean periodic flow:

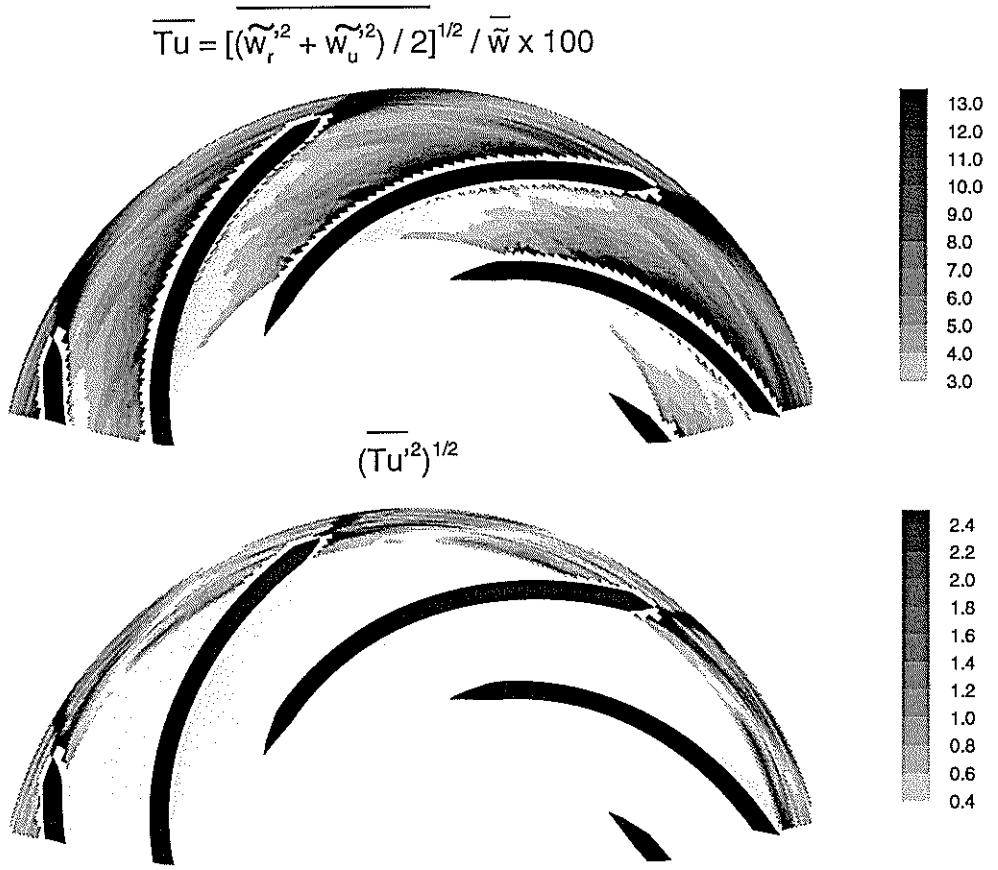

Fig. 6 Circumferentially averaged random unsteadiness and upstream diffuser effect on random unsteadiness

$$\bar{\tilde{c}}(t_j) = \sum_{k=1}^{K} \tilde{c}(t_j, \vartheta_k)\, \Delta\vartheta_k \,/ \sum_{k=1}^{K} \Delta\vartheta_k$$

Root mean square of the velocity fluctuations respect to the circumferentially averaged velocity is representative of the upstream potential effect of the diffuser on the impeller periodic outflow and, therefore, has been indicated as stator generated unsteadiness:

$$\sqrt{\overline{\tilde{c}'^2(t_j)}} = \sqrt{\sum_{k=1}^{K} \left[\tilde{c}(t_j, \vartheta_k) - \bar{\tilde{c}}(t_j)\right]^2 \Delta\vartheta_k \,/ \sum_{k=1}^{K} \Delta\vartheta_k}$$

The above procedure is repeated for all radial positions and the results are used to construct grey filled contour plots.

Figure 5 shows the distributions in the blade-to-blade plane of the non dimensional circumferentially averaged relative velocity $\bar{\tilde{w}} / U_2$ and stator generated unsteadiness $\left(\overline{\tilde{w}'^2}\right)^{1/2} / U_2$. The impeller rotation is counter clockwise.

At the nominal operating point the relative flow in the impeller is smooth and regular with maximum deceleration on the pressure side near mid-chord. The presence in the trailing edge region of a clear and a dark trace indicates that the flow rotates around the blade trailing edge, accelerating on the pressure side, and the viscous flow separates from the trailing edge suction side giving rise to the blade wake. The stator generated unsteadiness is less than 5 per cent, when referred to the peripheral velocity U_2 (about 10 per cent of the mean relative velocity) in most of the flow field, and rapidly decays in the impeller passages. The largest values are found in the radial gap, especially in the trailing edge region, with maximum values on the two sides of the wake and minimum values along the centerline of it.

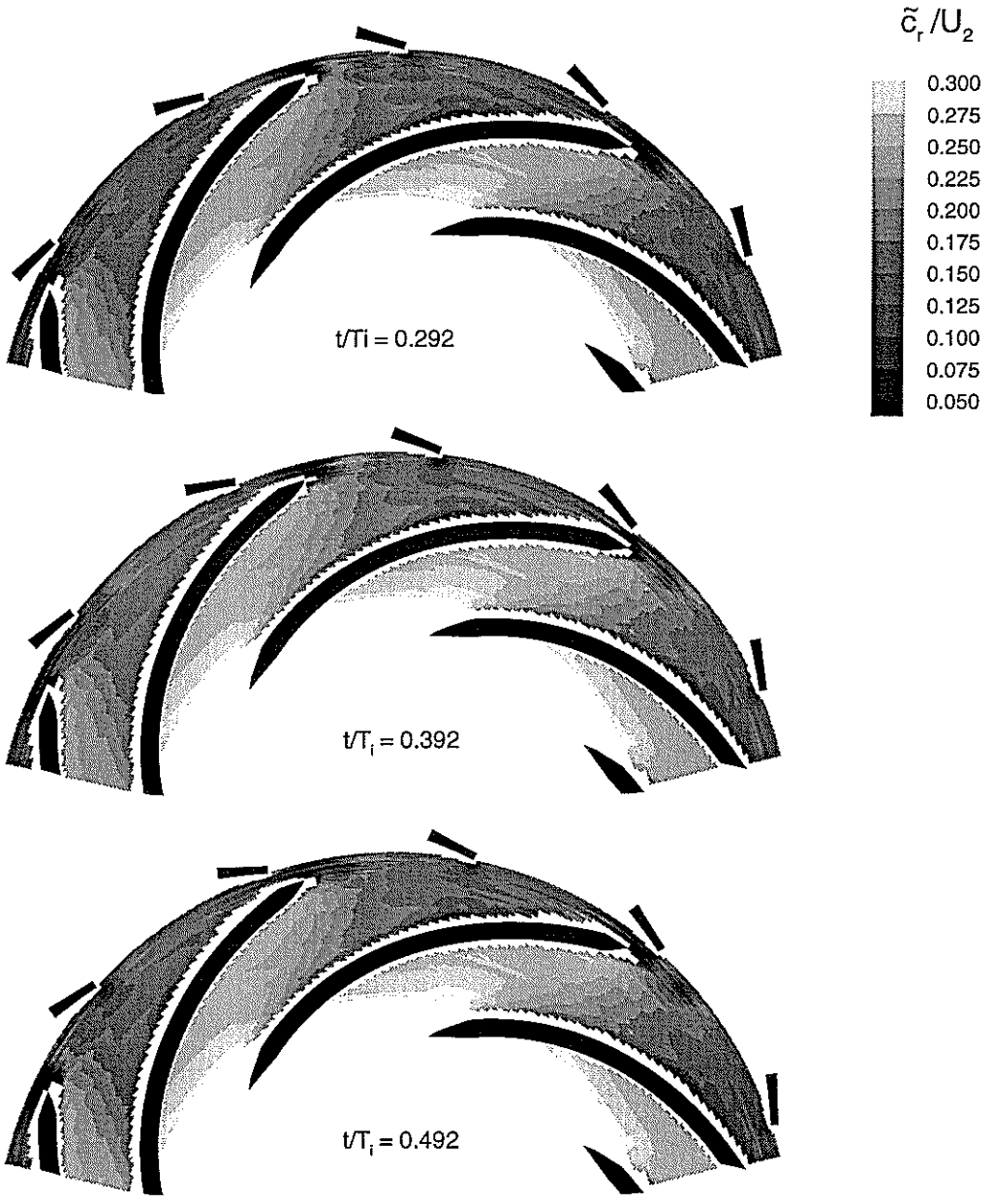

Fig. 7 Instantaneous distributions of ensemble averaged radial velocity component

The distributions of the circumferentially averaged unresolved unsteadiness $\overline{Tu}$, mainly due to turbulence, and its effective fluctuations induced upstream by the diffuser are shown in fig. 6. The turbulence is large, as expected in the wake region and also in proximity of the pressure side of the blade, where the flow deceleration promotes the boundary layer growth. In these regions the low values of the local relative velocity contribute to increase the values of $\overline{Tu}$, because of the normalisation adopted. The upstream diffuser effect on the turbulence looks qualitatively similar to the effect on the relative velocity.

Instantaneous distribution of the ensemble averaged velocity components

An alternative way to describe the potential flow effect of the vaned diffuser on the impeller outflow is to reconstruct a sequence of images of the flow field at fixed time instants. This objective can be achieved by reordering the information contained in the ensemble averaged distributions obtained for the 24 different circumferential positions ϑ_k of the diffuser vanes with respect to the probe volume.

To reconstruct the velocity distribution along a circumferential coordinate y in the relative reference frame at the time instant $t = \bar{t}$, it is necessary to interpolate the distribution of the velocity measured for different values of ϑ_k. We assume that the probe volume is located at y=0 for t = 0. At $t = \bar{t}$ the probe volume position is $y = \omega r \bar{t}$. The relative position between impeller and diffuser obtained at the time $t = \bar{t}$ with diffuser angular

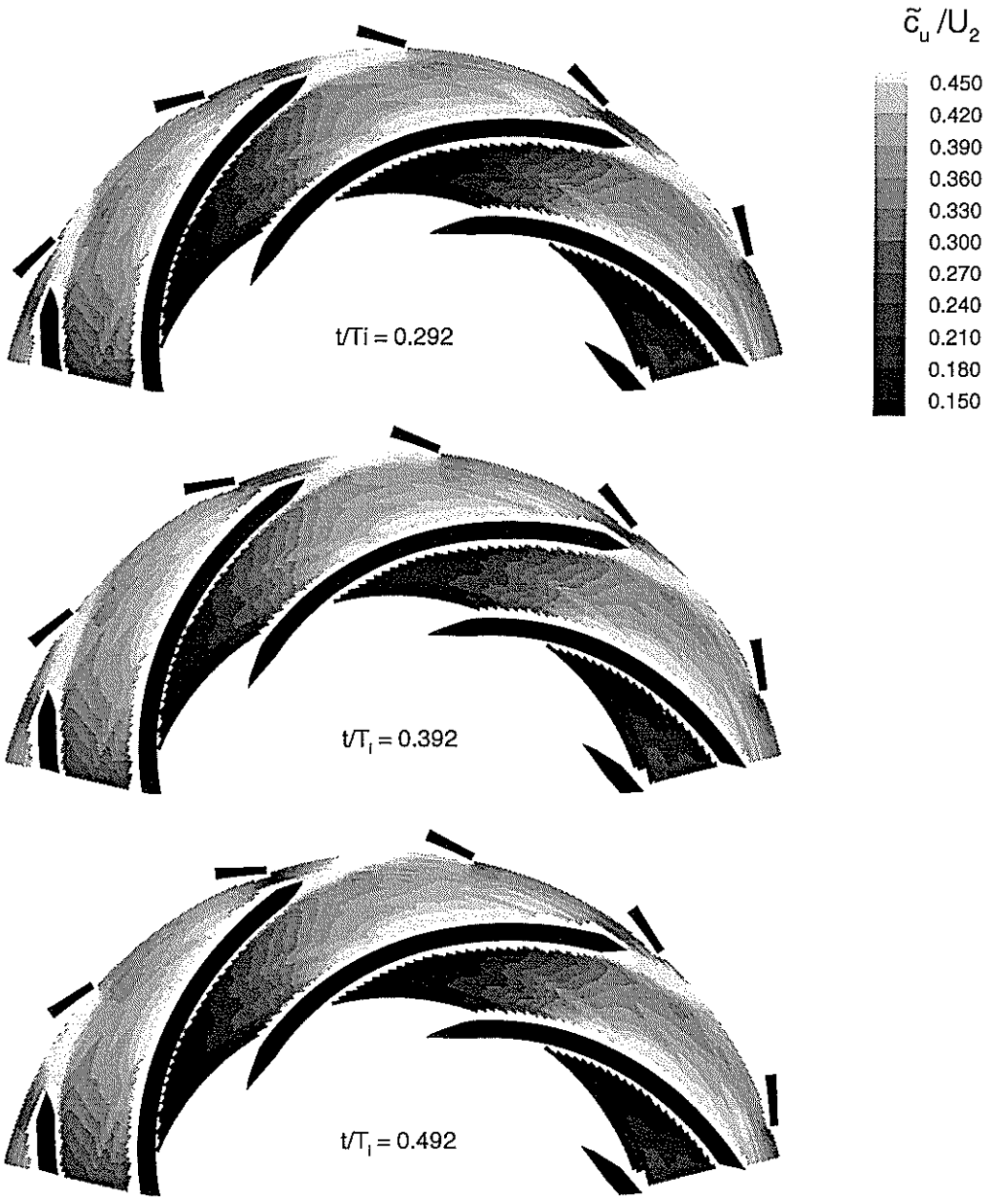

Fig. 8 Instantaneous distributions of ensemble averaged circumferential absolute velocity component

setting $\vartheta = 0$ is obtained at the time $t = \bar{t} + \vartheta_k / \omega$ if $\vartheta = \vartheta_k$ (the angular coordinate ϑ is assumed positive in the same direction of the impeller rotation). At this time instant the probe volume position in the relative frame is $y = \omega r \bar{t} + r\vartheta_k$

Therefore, all the K ensemble averaged velocity distributions can be interpolated in time to find the distribution in space of the velocity components. The procedure is repeated for all the radial positions investigated.

A sequence of images of radial and tangential absolute velocity components obtained for $t / T_i = 0.292$, 0.392 and 0.492 is given in figs. 7 and 8. In this representation the impeller appears fixed in time, while the diffuser vanes are seen to move clockwise.

The presence of the diffuser vanes influences the upstream flow. An important effect is the blockage on the radial velocity in proximity of the vane leading edge and the slight flow acceleration on the two sides of the vane. Contemporaneously the upstream flow is deflected by the diffuser vanes, with an increase of the tangential absolute velocity in the region adjacent to the suction side of the vane and a decrease of this velocity component near the vane pressure side.

These flow phenomena move jointly with the diffuser vanes at the angular velocity -ω with respect to the impeller, inducing a periodic perturbation on the steady relative flow with a period $T_d = T_i z_i / z_d = 0.58 T_i$.

These perturbations tend to enhance or depress the local non-uniformities of the relative flow, depending on the relative position in the impeller flow field, and attenuate rapidly within the impeller passages.

CONCLUSIONS

A non-intrusive laser Doppler technique has been used to study the details of the flow in the blade-to-blade plane set at mid-span in the radial gap between a centrifugal impeller and a vaned diffuser and within the rotor impeller passages.

Data from the counter processor analog output were continuously sampled and a software routine was developed to identify information pertaining to the actual passing of seeding particles in the probe volume and to calculate the corresponding arrival times.

The signals in phase with the impeller rotation were ensemble averaged to separate random and periodic fluctuations.

The upstream effect of the vaned diffuser on the impeller outflow has been investigated in the absolute reference frame by performing measurements for different circumferential positions of measuring point and vaned diffuser.

Two different data processing procedures have been applied to this extensive set of data. By circumferentially averaging the ensemble averaged distributions, a mean representative periodic flow has been produced and a stator induced unsteadiness on the impeller outflow has been identified and evaluated. By organising in time and space all the ensemble averaged data, sequences of images of the flow have been reconstructed, which show the instantaneous effect of the periodic flow perturbation induced by the diffuser.

At the nominal operating point, the upstream diffuser effect was found to decay very rapidly, nevertheless some interesting features have been observed and the developed measuring and data processing techniques have been proved to be suitable for the study of these unsteady phenomena.

More advanced laser Doppler instrumentation will be employed to extend the present investigation to cross sectional planes.

ACKNOWLEDGEMENTS

The work has been carried out with the support of M.U.R.S.T. The authors are also grateful to Riva Hydroart S.p.A., Milan, for having supplied the laser velocimeter within a common research program on turbomachinery internal flow.

REFERENCES

[1] Dring, R. P., Joslyn, H. D., Hardin, L. W., and Wagner, J. H., "Turbine Rotor-Stator Interaction", ASME *Journal of Engineering for Power*, Vol. 104, pp. 729-742, 1982.

[2] Pfeil, H., Herbst, R., and Schroeder, T., "Investigation of the Laminar-Turbulent Transition of Boundary Layers Disturbed by Wakes", ASME *Journal of Engineering for Power*, Vol. 105, pp. 130-137, 1983.

[3] Binder, A., Forster, W., Kruse, H., and Rogge, H., "An Experimental Investigation Into the Effect of Wakes on the Unsteady Turbine Rotor Flow", ASME *Journal of Engineering for Gas Turbines and Power*, Vol. 107, pp. 458-466, 1985.

[4] Hodson, H. P., "Measurements of Wake-Generated Unsteadiness in the Rotor Passages of Axial Flow Turbines", ASME *Journal of Engineering for Gas Turbines and Power*, Vol. 107, pp. 467-476, 1985.

[5] Suder, K. L., Hathaway, M. D., Okiishi, T. H., Strazisar, A. J., and Adamczyk, J. J., 1987,. "Measurements of the Unsteady Flow Field Within the Stator Row of a Transonic Axial-Flow Fan Part I and II", ASME Papers No. 87-GT-226 and 87-GT-227, 1987.

[6] Zeschky, J., and Gallus, H. E., "Effects of Stator Wakes and Spanwise Nonuniform Inlet Conditions on the Rotor Flow of an Axial Turbine Stage", ASME Paper No. 91-GT-93, 1991.

[7] Ubaldi, M., Zunino, P., Barigozzi, G., and Cattanei, A., "An Experimental Investigation of Stator Induced Unsteadiness on Centrifugal Impeller Outflow", ASME Paper No. 94-GT-5, 1994.

[8] Adrian, R. J., "Laser Velocimetry" in "Fluid Mechanics Measurements", Goldstein R. J. ed., pp. 155-240, Hemisphere, 1983.

[9] Dring, R. P., "Sizing Criteria for Laser Anemometry Particles", ASME *Journal of Fluid Engineering*, Vol. 104, pp. 15-17, 1982.

[10] Strazisar, A. J., Powell, J. A., "Laser Anemometer Measurements in a Transonic Axial Flow Compressor Rotor", ASME *Journal of Engineering for Power*, Vol. 103, pp. 430-437, 1981.

[11] Strazisar, A. J., "Laser Anemometry in Compressors and Turbines", ASME G. T. Division, Lectures on Fluid Dynamics of Turbomachinery, July 1986.